

An Adaptive Beam-Shaping Strategy for WCDMA Multicellular Networks with Non-Uniform Traffic Requirements

Panagiotis K. Gkonis¹, George V. Tsoulos², Georgia E. Athanasiadou² and Dimitra I. Kaklamani¹

¹National Technical University of Athens, Zografou, Greece

Emails: pgkonis@esd.ntua.gr, dkaklam@mail.ntua.gr

²University of Peloponnese, Tripoli, Greece

Emails: {gtsoulos,gathanas}@uop.gr

Abstract—This paper investigates the performance of an adaptive beam-shaping (ABS) strategy for wideband code division multiple access (WCDMA) multicellular networks with antenna arrays (AAs) at the base station (BS). The purpose of this ABS strategy is to form beams in directions of increased traffic distribution while at the same time minimize the total downlink transmission power. Performance is evaluated statistically with Monte Carlo (MC) simulations through a grid-enabled WCDMA system level simulator in terms of achievable throughput per beam for a network with up to four tiers of cells and increased loading (up to 90%). Results are presented for multirate services which show that the proposed ABS strategy can increase the throughput per beam relatively to a fixed grid of beams sectorization strategy up to 75/120/165% with 1/2/3 hotspots per cell respectively, while this gain is up to 35% for uniform traffic distribution. Moreover, it is shown that this gain can be achieved while at the same time the blocking probability in the central cell is reduced and the overall throughput of the network increased.

Index Terms — WCDMA, hotspot areas, adaptive beamforming, Monte Carlo simulations.

I. INTRODUCTION

The adoption of the WCDMA air interface as the physical layer protocol for third generation (3G) mobile networks led to higher transmission rates and more efficient spectrum utilization compared to second generation mobile networks. In WCDMA, different mobile stations (MSs) are separated in the time domain by multiplication of their signals with different spreading sequences. All MSs can transmit simultaneously occupying the whole transmission bandwidth ([1]). The desired signal can be acquired at the receiver through a convolution procedure with its spreading sequence.

However, the non-zero cross correlation of the spreading sequences in an asynchronous transmission environment gives rise to multiple access interference (MAI), which can degrade the performance of the network especially in cases of non-uniform traffic where an increased number of MSs is located in a small area.

In general, MAI can be suppressed in the signal domain with the use of appropriate multiuser detection techniques, in the spatial domain with the use of AAs at the BSs, or through appropriate admission control (AC) strategies which monitor the load in cells and decide on the acceptance of a potential MS according to the interference level in adjacent cells. Since capacity of 3G networks is mainly interference limited, the performance of different MAI suppression techniques can be evaluated only stochastically with extended MC simulations.

In [2], the authors developed a cellular model for system level investigations of AAs in WCDMA networks. Results were presented concerning the blocking probability for different network topologies and types of AAs. In [3], a directional power-based AC strategy was presented taking into account interference among adjacent beams. In [4], a partially adaptive approach with respect to fixed beamforming was adopted where two grouping and beam-shaping algorithms were presented and evaluated.

Other studies have focused on the performance of WCDMA networks with non-uniform traffic distribution (hotspot areas). In [5], the authors developed a theoretical model for the reverse link of a WCDMA network with hotspot areas where the BSs employ conventional 120° sectors. Results were presented concerning the maximum allowed interference level in a hotspot area region for acceptable quality of service. In [6], an adaptive sectorization strategy was proposed and evaluated for WCDMA networks with hotspot areas where performance metrics were derived concerning the blocking probability versus the dimensions of the hotspot area. In [7], a suboptimal adaptive cell sectoring solution to the optimal cell sectoring algorithm was presented along with results for a single cell environment and non-uniform traffic.

In all the above studies however, either limited network deployments were assumed (i.e. up to two tiers of cells around the central cell), or medium loading in sectors. Moreover, statistical rather than deterministic propagation models were employed.

In [8], an adaptive beam-centric AC strategy was presented and evaluated in terms of achievable throughput per beam for various network configurations and services.

This paper is based on "An adaptive admission control strategy for WCDMA multicellular networks with non-uniform traffic" by P.K. Gkonis, G.V. Tsoulos and D.I. Kaklamani which appeared in the Proceedings of the 66th Vehicular Technology Conference (VTC 2007-Fall), Baltimore, MD, USA, October 2007. © 2007 IEEE.

In this study, adaptive beams were formed according to traffic demands and system capacity was optimized through an AC/beamforming/optimization procedure. Results indicated that significant throughput per beam gain could be achieved for small hotspot area angular width and high data rate services. However, beamforming was performed with lobes of fixed beamwidth and no beamshaping according to traffic demands. This paper extends work in [8] for high loading factor scenarios where a joint beamforming/beamshaping procedure is presented and evaluated. Up to four tiers of cells are considered here and intercell interference is modeled with the help of a grid-enabled WCDMA system level simulator that executes independent MC simulations in parallel ([9]).

The rest of this paper is organized as follows: In section II the WCDMA system model is described along with the employed ray-tracing propagation model. In section III the WCDMA system level simulator is presented and in section IV the beamforming concepts are outlined along with the proposed ABS strategy. Results are presented and discussed in section V, while concluding remarks are made in section VI.

II. SYSTEM MODEL

System level simulations are performed in a network with up to four tiers of cells. It is assumed that the sectors up to the first tier of cells can employ AAs of M elements. All other sectors employ conventional 120° sectors with radiation patterns as specified in [10]:

$$f(\varphi) = G_b - \min \left[12 \left(\frac{\varphi - \varphi_s}{\varphi_{3dB}} \right)^2, A_m \right] \quad (1)$$

for $\varphi_s - 60^\circ \leq \varphi \leq \varphi_s + 60^\circ$. In (1), $\varphi_s \in \{90^\circ, 210^\circ, 330^\circ\}$ is the pointing direction of the sector, the antenna gain G_b equals 14dBi, the 3-dB beamwidth of the antenna pattern (φ_{3dB}) is 70° , and the front-to-back ratio (A_m) is 20dB.

An MS is connected to the BS with the lowest path loss (including shadowing). For the users outside the central cell pathloss is modeled as a sum of a deterministic term and a stochastic part. The deterministic term is defined for urban areas according to the Okumura-Hata model with a BS height of 30m, an MS height of 1.5m, and a carrier frequency of 2 GHz [11]:

$$PL_{OH}(dB) = 137.4 + 35.2 \log_{10}(R) \quad (2)$$

where PL_{OH} is the path loss and R is the range in km. The stochastic part which models the shadowing effect is comprised by a zero-mean Gaussian random variable in dB, with typical standard deviation of 8 dB for urban macrocellular environments.

However, in an attempt to increase accuracy, for the MSs in the central cell the pathloss is calculated with the use of deterministic propagation modeling. The ray tracing model employed in this paper [12] puts emphasis on modelling macrocellular operational environments, and hence, roof top diffraction is fully supported both

before and after reflections, since it is the dominant propagation mechanism when antennas are positioned on building tops or high on the external walls. The model works with raster terrain as well as 3D vector building and foliage databases. It also takes into account reflections off building walls, off-axis roof top and terrain diffractions and calculates the attenuation of each ray when it passes through foliage. The field of each ray found by the 3D ray-tracing algorithm is calculated according to the Uniform Theory of Diffraction and Geometrical Optics. Furthermore, the first Fresnel zone of each ray is examined and the losses due to its partial blockage are taken into account.

The digital geographical database of the simulated area shown in figure 1 is a typical urban city environment of $\sim 20 \text{ km}^2$ and the shaded area shows the approximate area of possible positions for central cell users.

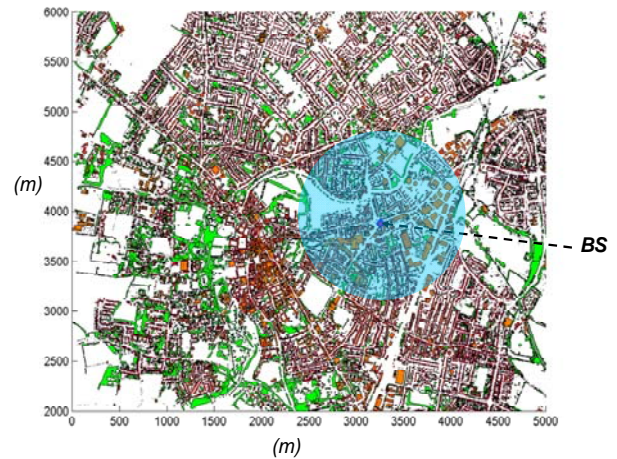


Fig 1. The studied macrocellular operational environment.

III. WCDMA SYSTEM LEVEL SIMULATOR

In all simulation scenarios it is assumed that users attempt to access the network at a sequential manner with a predefined traffic distribution. A user is admitted to the j^{th} sector if the following AC criteria are satisfied:

$$\mathbf{I}_{sectors}(j) + \Delta I \leq I_{sectors_max} \quad (3)$$

$$P_{d,j} + \Delta P \leq P_{th} \quad (4)$$

$$p_u \leq p_{u_max} \quad (5)$$

$$p_d \leq p_{d_max} \quad (6)$$

In (3) and (4), $\mathbf{I}_{sectors}(j)$ is the total received power from the j^{th} sector, $P_{d,j}$ is the total transmission power of the j^{th} sector, ΔI and ΔP are the estimated increases in the received power of the j^{th} sector and its total transmission power respectively caused by the potential MS, $I_{sectors_max}$ is the maximum allowed received power in a sector and P_{th} its maximum allowed transmission power. In (5) and (6), p_u and p_d are the up and downlink transmission powers of the potential active MS respectively and finally p_{u_max} and p_{d_max} are the up and downlink maximum allowed transmission powers per MS respectively.

After the entrance or removal of a MS, power control in the up and downlink is performed and transmission powers are updated. The purpose of power control is to maintain all MS's Signal to Interference plus Noise Ratio (*SINR*) above a predefined threshold for acceptable quality of service. For a given service (i.e. voice or data services), the *SINR* for the i^{th} MS with the q^{th} service which is served by the j^{th} sector is given by:

$$SINR_q = \frac{S_{q,i}}{\mathbf{I}_{sectors}(j) - S_{q,i}} \quad (7)$$

where $S_{q,i}$ is the power received from the i^{th} MS. Note that if all MSs in the j^{th} sector have common service then the received powers $S_{q,i}$ will be equal for all MSs in this sector. Hence, in order to reduce the complexity of the calculations, the received powers of the sectors can be calculated by solving a linear $K \times K$ system of equations. The received power from the j^{th} sector is given by:

$$\mathbf{I}_{sectors}(j) = \sum_{q=1}^U \sum_{n=1}^N \frac{L_{n,sector(n),q}}{L_{n,j,q}} S_{q,n} + I_n \quad (8)$$

where U is the number of services in the network, N is the total number of MSs, $L_{n,j,q}$ denotes the total losses of the n^{th} MS with the q^{th} service belonging to *sector*(n) relevant to the j^{th} sector (including shadowing and antenna radiation patterns) and I_n is the thermal noise. Note that $S_{q,n}$ is the received power from the n^{th} MS with respect to his serving sector. By grouping MSs according to their serving sector and service, (8) can be written as:

$$\mathbf{I}_{sectors}(j) = \sum_{i=1}^K \sum_{q=1}^U \sum_{n=1, n \in i}^N \frac{L_{n,i,q}}{L_{n,j,q}} S_{q,i} + I_n \quad (9)$$

By denoting $\mathbf{T}_q(i, j) = \sum_{q=1}^U \sum_{n=1, n \in i}^N \frac{L_{n,i,q}}{L_{n,j,q}}$ and in conjunction with (7) and (8), (9) can be written as:

$$\mathbf{I}_{sectors} = \left(\sum_{q=1}^U \mathbf{T}_q \frac{SINR_q}{1 + SINR_q} \right) \mathbf{I}_{sectors} + I_n \quad (10)$$

which can be solved directly for $\mathbf{I}_{sectors}$:

$$\mathbf{I}_{sectors} = \left(\mathbf{I} - \left(\sum_{q=1}^U \mathbf{T}_q \frac{SINR_q}{1 + SINR_q} \right) \right)^{-1} I_n \quad (11)$$

where \mathbf{I} is the $K \times K$ identity matrix.

In the downlink, the required transmit power per MS is given by ([13]):

$$p_i = \left(\frac{E_b}{N_o} \right)_i \frac{R_i}{W} \left((1 - \alpha_i) P_{d,m} + \sum_{j=1, j \neq m}^K P_{d,j} \frac{L_{i,m,q}}{L_{i,j,q}} + I_n L_{i,m,q} \right) \quad (12)$$

where m is the serving sector of the i^{th} MS, R_i is the bit rate, W is the chip rate and α_i is the orthogonality factor ($\alpha_i=1$ for the case of a single propagation path). In the rest of the paper it is assumed that α_i is common for all MSs in the network.

If the power calculated by (12) does not exceed the maximum allowed downlink transmission power per MS, then the E_b/N_o requirement for acceptable quality of service for the i^{th} MS is satisfied. The total downlink transmission power for the j^{th} sector is given by:

$$P_{d,j} = \sum_{i=1, i \in j}^N p_i + P_{com} \quad (13)$$

where P_{com} is the power allocated for the transmission of the common channels. It follows from (13) that the transmission power of the j^{th} sector can be expressed as a linear weighted sum of the other sectors' transmit powers. Hence, by denoting \mathbf{P} the vector of the downlink transmission powers, it can be calculated by:

$$\mathbf{P} = \mathbf{C}^{-1} \mathbf{D} \quad (14)$$

where the matrices \mathbf{C} and \mathbf{D} are given by:

$$C(i, j) = -1 + \sum_{k=1, k \in i}^N \left(\frac{E_b}{N_o} \right)_k \frac{R_k}{W} \left\{ (1 - \alpha) \delta_{ij} + \frac{L_{k,i,q}}{L_{k,j,q}} (1 - \delta_{ij}) \right\} \quad (15)$$

$$D(i, j) = P_{com} + \sum_{k=1, k \in i}^N \left(\frac{E_b}{N_o} \right)_k \frac{R_k}{W} I_n L_{k,i,q} \quad (16)$$

where δ is the Kronecker delta. If after the power control procedure the received power in an effective sector or its downlink transmission power are above their maximum allowed values, or a MS needs to transmit more than its maximum allowed up or downlink transmission power, then MSs are removed from the network until interference levels in all effective sectors and transmission powers are below their maximum allowed values. If $\mathbf{I}_{sectors}(j) > I_{sectors,max}$ or $P_{d,j} > P_{d,max}$ is true for the j^{th} sector, then the n^{th} MS is removed according to:

$$n = \max_{1 \leq n' \leq N} \left\{ \frac{P_{u,n'}}{L_{n',j,q}} \right\} \cup \max_{1 \leq n' \leq N} \left\{ \frac{P_{d,n'}}{L_{n',j,q}} \right\} \quad (17)$$

After completion of this process, power control is performed and the process is repeated until all interference levels and transmission powers are below their maximum allowed values.

IV. BEAMFORMING CONCEPTS AND ADAPTIVE BEAM-SHAPING STRATEGY

A. The Beamforming Procedure

In this paragraph the beamforming concepts are described for the formulation of fixed or dynamic radiation patterns. It is assumed that the BSs up to the first tier of cells can employ AAs of M elements, able to form a maximum number of $M-1$ orthogonal beams, in order to reduce interbeam interference. The composite array factor (AF) in dB for the m^{th} beam is given by:

$$AF_m = f(\varphi) + 20 \log_{10}(S_m(\varphi)) \quad (18)$$

where $S_m(\varphi)$ is the array factor of the m^{th} beam satisfying:

$$S_m(\varphi_n) = \delta_{mn} \quad (19)$$

In (19) φ_n is the pointing direction of the n^{th} beam. The produced radiation patterns are formed dynamically according to traffic demands. By denoting K_i the number of beams produced by i elements of the AA ($i \leq M$) with common beamwidth Δ_i , then:

$$\sum_i K_i \leq M - 1 \quad (20)$$

The left term of (20) is maximized when $i=M$. The weight vector for the j^{th} beam can be calculated by ([14]):

$$\mathbf{w}^H = \mathbf{e}^T \mathbf{A}^H (\mathbf{A} \mathbf{A}^H)^{-1} \quad (21)$$

where $[.]^H$ denotes the conjugate transpose of a matrix, \mathbf{w} is the desired weight vector, \mathbf{A} is a matrix with columns the steering vectors associated with all directional sources, (including the look direction), and \mathbf{e} is a vector with all the elements zeros except from the j^{th} element which equals to one. The steering vector in a direction φ_j for an antenna element separation $\lambda/2$ and the antenna array in the x-axis is ([14]):

$$\mathbf{s}_j = [1, \exp(j\pi \cos(\varphi_j)), \dots, \exp(j\pi(i-1) \cos(\varphi_j))]^T \quad (22)$$

The multipath propagation seen at the BS can be modeled either analytically with the use of the ray tracing model or statistically with the use of a predefined angular spread distribution. For the MSs in central cell, the modified radiation patterns which take into account multipath propagation and pathloss are given by:

$$G_m(\phi) = \sum_{i=1}^Q |AF_m(\phi_i)|^2 PL_{RT}^i \quad (23)$$

where Q is the total number of multipath components, PL_{RT}^i is the pathloss of the i^{th} multipath and ϕ_i its angle of departure. Both AF_m and PL_{RT} are in scalar values.

In the statistical approach, the power azimuth spectrum at the BS is assumed to follow a Laplacian distribution with an azimuth spread of 5° for typical urban environments ([15]):

$$G_m(\phi) = \left(\int_{-\pi}^{\pi} |AF_m(\phi')|^2 p_A(\phi' - \phi) d\phi' \right) PL_{OH} \quad (24)$$

where PL_{OH} is as defined in (2) in scalar values and $p_A(\phi)$ is the Laplacian distribution.

B. The Adaptive Beam-Shaping Strategy

In all simulation scenarios as it will be explained in section V, three types of services are considered: voice services of 12.2 Kbps and data services of 144/384 Kbps respectively. Beamforming is performed with priority to high data rate MSs. In the initial state, all sectors employ conventional 120° sectors. If a high data rate MS tries to access the network in the central cell or in the first tier of cells around the central cell, beamforming takes place where a directional beam with beamwidth Δ_M is formed pointing to the high data rate MS. Afterwards, a pattern-filling procedure is performed in the right and left angular space of the produced beam (i.e. the angular space defined between the pointing direction of the beam and the minimum/maximum angle of the sector respectively) in order to provide coverage to all other potential MSs in the sector. This procedure is described in the following for the right angular space, where it is assumed that the maximum beamwidth of an adaptive beam is Δ_3 . Moreover, AoA denotes the angle of arrival of the high data rate MS, i is the index of an adaptive beam and $angle$, $beamwidth$ are the vectors of the steering directions of the produced radiation patterns and their beamwidths respectively.

The Pattern-Filling Algorithm

- **Step 1:** Initialization, set $i=1$,
 $angle(i) \leftarrow AoA$,
 $beamwidth(i) \leftarrow \Delta_M$,
 $min_angle \leftarrow 30^\circ$, $max_angle \leftarrow 150^\circ$
- **Step 2:** Define
 $\Delta\varphi \leftarrow angle(i) - beamwidth(i)/2 - min_angle$
and $j \leftarrow \min_{3 \leq j \leq M} \|\Delta_j - \Delta\varphi\|$
- **Step 3:** If $\Delta\varphi > \Delta_j$ set
 $i \leftarrow i + 1$
 $angle(i) \leftarrow angle(i-1) - \Delta_j/2 - beamwidth(i-1)/2$
 $beamwidth(i) \leftarrow \Delta_j$
Then go to step 2.
- **Step 4:** If $\Delta\varphi < \Delta_j$ then repeat:
 $j \leftarrow j + 1$
until $\Delta_j < \Delta\varphi$ or $j < M-1$
Go to step 5.
- **Step 5:** If $\Delta\varphi > \Delta_j$ go to step 2 else the procedure terminates.

In step 2, the angular space between the minimum angle of the sector which is 30° and the AoA of the high data rate MS is defined. The purpose is to form a directional beam with beamwidth Δ_M pointing to the high data rate MS and at the same time form less directional beams to cover the entire right angular space. The above procedure is then repeated for the left angular space.

For every other MS to access the network in the central cell or in the first tier of cells around the central cell, it is examined first if it can be allocated to one of the already existing beams. If the potential MS is not a high data rate MS, then it is allocated to the j^{th} beam if the condition $|AoA - \varphi_j| < \text{beamwidth}(j)/2$ is satisfied. However, high data rate MSs can be allocated only to directional beams with beamwidth Δ_M . If the potential MS cannot be allocated to one of the already existing beams and it is a high data rate MS, then a new directional beam can be formed according to ([8]):

$$\varphi = \begin{cases} AoA, & \text{if } |AoA - \varphi_{1,2}| > \Delta_M \\ \varphi_1 + \Delta_M, & \text{if } |AoA - \varphi_1| < \Delta_M < |\varphi_1 + \Delta_M - \varphi_2| \\ \varphi_2 - \Delta_M, & \text{if } |AoA - \varphi_2| < \Delta_M < |\varphi_2 - \Delta_M - \varphi_1| \\ \varphi_{\min} + \Delta_M / 2, & \text{if } |AoA - \varphi_{\min}| < \Delta_M / 2 \\ \varphi_{\max} - \Delta_M / 2, & \text{if } |AoA - \varphi_{\max}| < \Delta_M / 2 \end{cases} \quad (25)$$

In (25) φ is the pointing direction of the new beam, $[\varphi_{\min}, \varphi_{\max}]$ denotes the sector beamwidth and φ_1 and φ_2 are the pointing directions of two consecutive beams with beamwidth Δ_M and $\varphi_1 < \varphi_2$. If neither a new beam can be formed towards the potential MS nor can it be grouped to an already existing beam, then this MS is rejected.

Note that if a new beam with beamwidth Δ_M is formed, then the pattern filling procedure described previously is repeated by setting $\text{min_angle} = \max\{\varphi_1 + \Delta_M/2, \varphi_{\min}\}$ and $\text{max_angle} = \min\{\varphi_2 - \Delta_M/2, \varphi_{\max}\}$.

C. The Pattern-Optimization Procedure

After beamforming, an optimization procedure takes place where beams of high data rate MSs are steered to the directions which minimize the total downlink transmit power. Note from that (12) the total downlink transmission power of the m^{th} beam can be expressed as:

$$P_m = \frac{\sum_{i=1}^{N_m} \left(\left(\frac{E_b}{N_o} \right)_i \frac{R_i}{W} \left(L_{i,m,q} \left(\sum_{j=1}^{K_1} \frac{P_{d,j}}{L_{i,j,q}} + \sum_{k=1}^{K_2} \frac{P_{d,k}}{L_{i,k,q}} + I_n \right) \right) \right)}{1 - (1-a) N_m \left(\frac{E_b}{N_o} \right)_i \frac{R_i}{W}} \quad (26)$$

where K_1 denotes the set of sectors employing adaptive beams and K_2 the set of conventional sectors. Moreover, N_m is the number of MSs in the m^{th} beam. Note from (26) that the losses $L_{i,m,q}$ and $L_{i,j,q}$ depend on the steering directions of the adaptive beams belonging to K_1 while the losses $L_{i,k,q}$ are constant since the directivity of the sectors in K_2 is predefined.

All angles φ_m are set initially so as to minimize P_m . However, changes of φ_m might impact on the downlink transmission power of another effective sector. Hence downlink power control is performed and the procedure is repeated until there are no changes in the downlink transmission powers of all effective sectors.

The optimization procedure is described in the following where k denotes the repetition index and $\varphi_{k,m}$, $P_{k,m}$ are the steering direction of the m^{th} beam and its downlink transmit power respectively at the k^{th} iteration.

The Beam-Optimization Algorithm

- **Step 1:** Initialization: set $k=1$.
- **Step 2:** By keeping $\varphi_{k,n}$ for every $n \neq m$ constant, define $\varphi_{k,m}$ for every m as:

$$\varphi_{k,m} = \min_{\varphi_{\min} < \varphi < \varphi_{\max}} \left\{ \frac{\sum_{i=1}^{N_m} \left(\left(\frac{E_b}{N_o} \right)_i \frac{R_i}{W} \left(L_{i,m,q}(\varphi) \left(\sum_{j=1}^{K_1} \frac{P_{d,j}}{L_{i,j,q}} + \sum_{k=1}^{K_2} \frac{P_{d,k}}{L_{i,k,q}} + I_n \right) \right) \right)}{1 - (1-a) N_m \left(\frac{E_b}{N_o} \right)_i \frac{R_i}{W}} \right\}$$

- **Step 3:** If $|\varphi_{k,m} - \varphi_{k,n}| > \Delta_M$ for every m, n in K_1 then go to step 8, else go to step 4.
- **Step 4:** If $|\varphi_{k,m} - \varphi_{k,n}| < \Delta_M$ for the m^{th} and n^{th} beam, then a beam-shaping procedure takes place. Beams m, n are merged in a common beam with beamwidth $2\Delta_M$.
- **Step 5:** If blocking occurs in the m^{th} beam with beamwidth $2\Delta_M$, then two new beams of beamwidth Δ_M are formed with pointing directions $\varphi_m - \Delta_M/2$ and $\varphi_m + \Delta_M/2$ respectively and the new optimum angles for these beams are calculated as in step 2. If these angles are equal to $\varphi_m - \Delta_M/2$ and $\varphi_m + \Delta_M/2$, respectively, then go to step 8 else go to step 6.
- **Step 6:** A new beam with beamwidth Δ_M is formed. A subset of the N_m MSs of the initial beam with beamwidth $2\Delta_M$ is selected in the angular space $[\varphi_m - \Delta_M/2, \varphi_m + \Delta_M/2]$, which minimizes the total downlink transmit power of the new beam. Go to step 7.
- **Step 7:** Two new beams are formed with beamwidth Δ_M in directions $\varphi_m - \Delta_M$ and $\varphi_m + \Delta_M$ respectively in order to cover the MSs that were excluded from the previous step, where the beamwidth of the produced beam was reduced to half.
- **Step 8:** The pattern-filling procedure is performed for the m^{th} beam if $\varphi_{k,m} \neq \varphi_{k-1,m}$. Power control in the downlink is performed and the transmission powers $P_{k,m}$ are updated.
- **Step 9:** If $\left| \frac{P_{k,m} - P_{k-1,m}}{P_{k-1,m}} \right| > 10^{-3}$ for the m^{th} sector then go to step 2, else the optimization process is terminated.

The optimization procedure described above finally steers a directional beam towards the area of increased traffic distribution. Consider for example that such an area exists in the angular space $[\varphi - \Delta_{hotspot}/2, \varphi + \Delta_{hotspot}/2]$ of a sector, with $\Delta_{hotspot} = \Delta_M$. If the AoA of the first MS to arrive is φ , then the optimum directional beam will be steered towards this hotspot area and only steps 1, 2, 3, 8 and 9 of the above optimization procedure will be performed.

In the extreme scenario however, the AoAs of the first two high data rate MSs to arrive will be $\varphi_1 = \varphi + \Delta_{hotspot}/2$ and $\varphi_2 = \varphi - \Delta_{hotspot}/2$ respectively. Two new beams will then be formed pointing to the boundaries of the hotspot area. If another high data rate MS arrives within the above hotspot area, then it will be allocated to one of the two beams that are steered in the boundaries of the hotspot area, as the condition $|AoA - \varphi_{1,2}| < \Delta_M/2$ is satisfied for one of the two beams. However, the angle which minimizes the total downlink transmit power of the beam will be different from its pointing direction. The beam cannot be steered to the optimum angle, as there is another adjacent beam.

A temporary solution is given in step 4, where the two beams are merged in a common beam. However, the increased traffic distribution due to the hotspot area will eventually cause blocking in this beam. According to step 5, a new beam will be formed towards the direction of the hotspot area. Note in this case that splitting in two adjacent beams cannot be performed since the optimum angle coincides with the pointing direction of the initial beam. Moreover, since MSs are excluded from this new beam, note from step 7 that two new beams with beamwidth Δ_M are formed in order to cover all other MSs in the angular space of the previous beam.

However, if there is not enough angular space to form adjacent beams next to the beam pointing to the hotspot area, then the MSs that cannot be served by a beam will be removed from the network.

V. RESULTS

Results are presented in figures 2-9 according to the simulation scenarios and parameters described in table I. The E_b/N_o values for different services and different channel scenarios are as in [16]. The purpose of the MC simulations is to examine the performance of the ABS strategy under non-uniform traffic requirements. Therefore, two network topologies are considered: fixed grid of beams (FGoB) in the central cell or in the first tier of cells and adaptive grid of beams (AGoB) respectively, which is formed dynamically according to the ABS strategy described in the previous section. In both topologies the power-based AC criteria described in section III are applied.

Up to three hotspot areas are formed either in the central cell or in the first tier of cells around the central cell. Each hotspot area has range equal to cell range and angular width that varies between $0.25\Delta_M$ and $7\Delta_M$. Up to one hotspot area can be generated in a sector. Furthermore, once a MS is distributed in the central cell or in the first tier of cells, is further distributed in a

hotspot area region with probability that equals $p_{hot_spots} \times total_hot_spots$ where $p_{hot_spots} = 1/3$ and $total_hot_spots$ represents the total number of hotspots per cell. Note that for three hotspots the above probability equals to one; and hence all MSs are distributed within hotspots. As the hotspot area angular width increases then the distribution approaches uniform.

A. Throughput per beam gain

In figures 2-4 is shown the gain of the ABS strategy, (expressed as the ratio of the throughput per beam in the AGoB network to the throughput per beam in the FGoB network) for grid of beams (GoB) in the central cell or in the first tier of cells. For every simulation scenario, two values for the loading factor are considered: 50% and 90% which represent a medium/highly loaded network, respectively. Moreover, it is assumed that the BSs up to the first tier of cells can employ an AA of 8 elements per sector able to form up to 7 directional orthogonal beams.

As it can be observed from figures 2-4, the throughput per beam gain increases as the number of hotspot areas in the central cell or in the first tier of cells increases. In particular, the gain can be up to 50/95/145% for 50% loading, GoB in the central cell and 1/2/3 hotspots per cell, respectively, while it is up to 75/120/165% for GoB in the first tier of cells. As the number of hotspot areas increases, then for small hotspot area angular width there is increased spatial separation among MSs. Therefore, intracell interference is reduced and fewer directive beams are needed to cover capacity demands, thus increasing the throughput per beam gain.

In all non-uniform traffic scenarios, the throughput per beam gain is lower for 90% loading. According to the traffic distribution specified in table I, the 40% of the potential MSs that try to access the network are high data rate MSs (30% and 10% data services of 144 and 384 Kbps, respectively). Therefore, for low levels of acceptable interference (i.e. 3dB for 50% loading), the network is more vulnerable to intracell and intercell interference, as high data rate MSs require a higher amount of transmission power compared to voice services due to their lower processing gain. Hence, the network benefits more from the ABS strategy which forms directional beams pointing to the directions of high data rate MSs, thus reducing their transmission power and in turn reducing the levels of interference.

As it can be observed from figures 2-4, as the angular width of the hotspot area increases the gain decreases, since the spatial separation among MSs also decreases and consequently the interbeam interference increases. For hotspot area angular width equal to $7\Delta_M$, (i.e. uniform user distribution in a cell, since $7\Delta_M \approx 120^\circ$), the non zero value of the gain stems from the fact that the produced radiation patterns point to high data rate MSs and hence, the throughput in a beam is increased compared to the FGoB network, even though there are no hotspot areas. This gain is practically the same for different number of hotspots per cell, as the distribution is uniform. In particular, for 50% loading the throughput per beam gain can be up to 35% for the three traffic scenarios while for 90% loading it can be up to 20%.

Moreover, the gain is higher for the case of GoB in the first tier of cells. The relevant difference is more obvious for low hotspot angular width or number of hotspots per cell. For three hotspots per cell the differences in the gain among the two network topologies (GoB in central cell and in the first tier) are minor.

From the above it becomes apparent that the performance of the ABS strategy depends mainly on intracell rather than intercell interference. Note that for one hotspot per cell the GoB in the first tier of cells reduces intracell interference in the central cell and hence increases the throughput per beam gain. However, for small hotspot angular width and three hotspots per cell, intracell interference is practically zero in both network topologies due to the spatial isolation among the beams, and hence there are no significant differences in the achieved throughput per beam gain.

In figure 5, results are provided for the throughput per beam gain considering GoB in the central cell and 3 hotspots, for two different channel scenarios (Static and Case 3 as described in table I). As it can be observed there are minor differences in the gain of the ABS strategy among the two different channel scenarios. This is rather expected, as the same AC criteria that are applied in the FGoB network are also applied in the AGoB network. Therefore, all simulations were carried out with the E_b/N_o values of the static channel case.

TABLE I
SIMULATION PARAMETERS

Parameter	Assumption
Cell radius	800 m
Carrier frequency	2 GHz
BS height	30 m
MS height	1.5 m
Propagation	MSs in central cell: Ray – Tracing model MSs outside central cell: Okumura – Hata, pathloss exponent 3.5
Azimuth dispersion for MSs not in central cell	Laplacian distribution, azimuth spread 5°
Maximum power per MS(downlink)	29.3dBm
Maximum power per MS(uplink)	21 dBm (voice services of 12.2 kbps) 24 dBm (data services of 144 or 384 kbps)
Maximum power per BS	43 dBm
Power threshold per sector (P_{th})	38.2dBm (i.e. 20W/3)
Orthogonality factor	0.5 (Typical Urban)
Radiation pattern of the antenna element	Broadside gain = 14 dBi Front-to-back ratio = 20dB 3-dB beamwidth = 70°
Number of antenna array elements	8
Speech AMR 12.2 Kbps	Static(AWGN): E_b/N_o (uplink/downlink) = 5.1/5.6 dB Case 3: E_b/N_o (uplink/downlink) = 7.2/8.93 dB
Data PS 144 kbps	Static(AWGN): E_b/N_o (uplink/downlink) = 0.8/2.2 dB Case 3: E_b/N_o (uplink/downlink) = 2.8/4 dB
Data PS 384 kbps	Static(AWGN): E_b/N_o (uplink/downlink) = 0.9/2.1 dB Case 3: E_b/N_o (uplink/downlink) = 3.2/4.4 dB
Traffic scenario	Voice and data services (12.2/144/384 kbps) with distribution probability vector [0.6, 0.3, 0.1] respectively

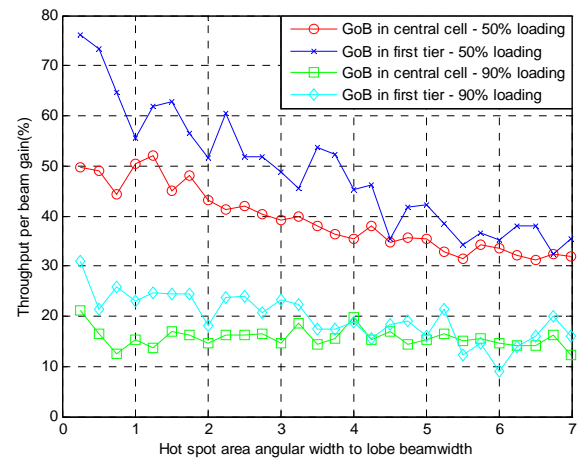


Fig 2. ABS strategy throughput per beam gain - 1 hotspot

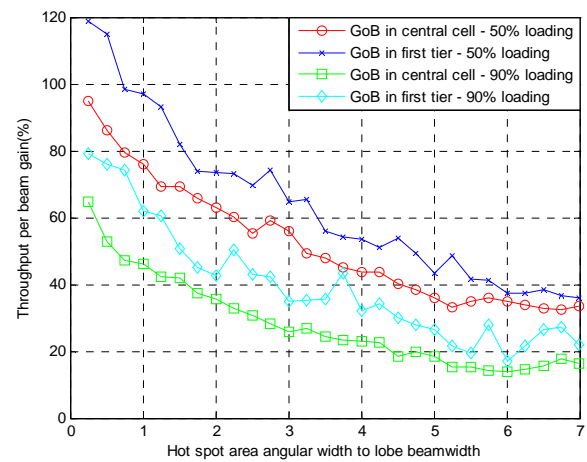


Fig 3. ABS strategy throughput per beam gain - 2 hotspots

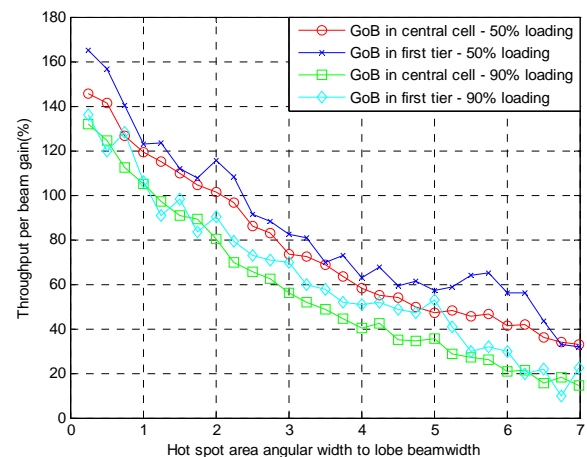


Fig 4. ABS strategy throughput per beam gain - 3 hotspots

B. Adaptive Beam-Shaping Strategy versus Adaptive Beam-Centric AC Strategy

In figures 6, 7, 8 and 9 the throughput per beam gain, the central cell throughput, the central cell blocking probability and the total network throughput respectively, are provided for GoB in the central cell and one hotspot area.

In all graphs there is a comparison of two different beamforming approaches: the ABS strategy presented in this paper and the adaptive beam-centric AC strategy presented in [8]. This beamforming strategy forms directional beams according to (25) with beamwidth Δ_M and no beam-shaping takes place. Furthermore, all MSs are treated equally regardless of their bit rate.

On the contrary, the ABS strategy forms directional patterns giving priority to high data rate MSs, while at the same time forms patterns with lower directivity in the areas of decreased traffic distribution in an attempt to reduce blocking probability.

The throughput per beam gain with the adaptive beam-centric AC strategy for low hotspot area angular width is higher compared to the throughput per beam gain with the ABS strategy. The relative difference decreases as the hotspot area angular width increases. As it can be observed from figure 6 the throughput per beam gain can be up to 50/77% with the ABS/adaptive beam-centric AC strategy respectively. However, this increase comes at the cost of increased blocking probability. From figures 7 and 8 it follows that the central cell blocking probability can be almost double with the adaptive beam-centric AC, although central cell's capacity is practically the same for both beamforming strategies.

In general, the adaptive beam-centric AC strategy forms fewer beams compared to the ABS strategy. For example, for hotspot area angular width less or equal to Δ_M and three hotspots per cell, only three directional beams with beamwidth Δ_M are formed in order to cover capacity demands. Hence, apart from increased throughput per beam gain this also provides significant reduction in the interbeam handovers, which in turn results in reduced signaling requirements from the network point of view. However, from a throughput point of view, blocking probability is increased as the pattern filling procedure is not performed and there can be angular spaces not covered by a beam; hence potential users in these areas will be likely rejected from the network.

The ABS strategy presented in this paper is an improved version of the adaptive beam-centric AC strategy, as for the same amounts of central cell's capacity it provides significantly reduced blocking probability. This probability is 9/17% for the ABS/adaptive beam-centric AC strategy respectively and uniform traffic distribution, as in this case MSs are distributed in the entire sector and the directional beams cannot provide sufficient coverage.

Finally, as it can be observed from figure 9 the total network throughput is increased in the ABS strategy (up to 700 Kbps) compared to the network throughput in the adaptive beam-centric AC strategy. Since directive beams are formed towards high data rate MSs, intercell MSs undergo lower amounts of interference and hence the overall capacity is increased.

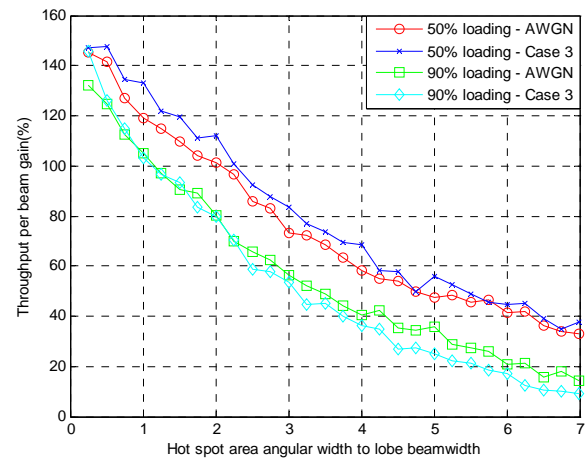


Fig 5. ABS strategy throughput per beam gain for the two different channel scenarios - 3 hotspots in central cell.

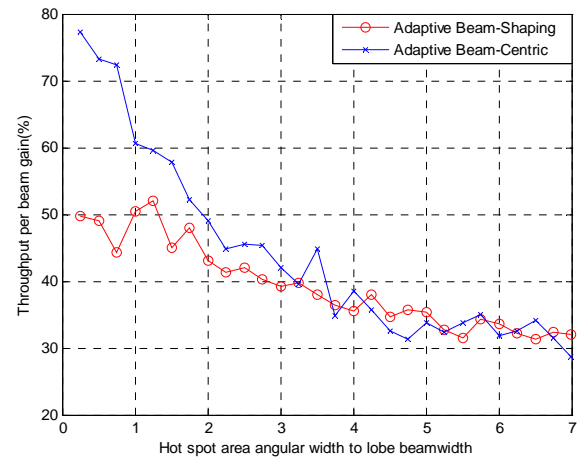


Fig. 6. Throughput per beam gain - Adaptive beam-centric AC strategy versus ABS strategy - 1 hotspot in the central cell.

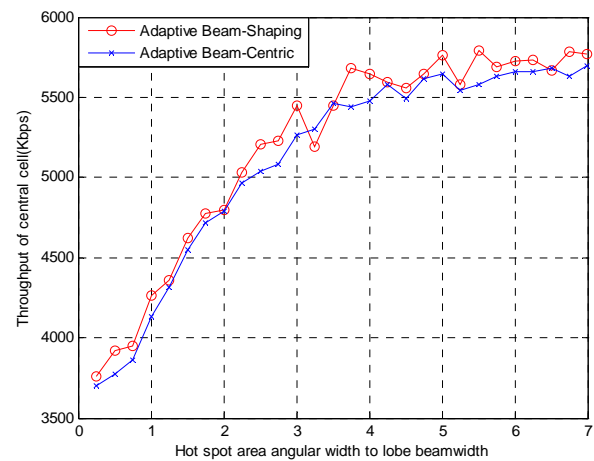


Fig. 7. Central cell throughput - Adaptive beam-centric AC strategy versus ABS strategy - 1 hotspot in the central cell.

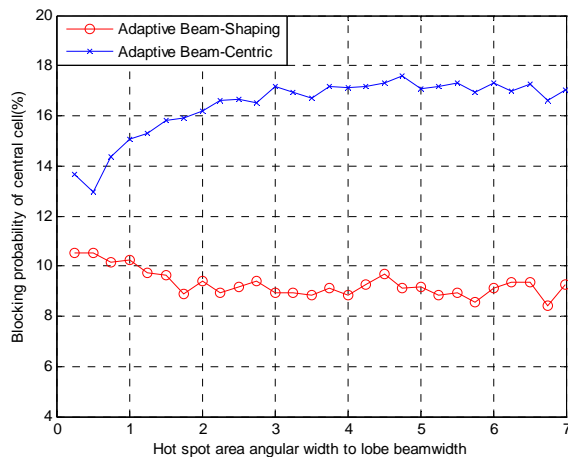


Fig 8. Central cell blocking probability - Adaptive beam-centric AC strategy versus ABS strategy - 1 hotspot in the central cell.

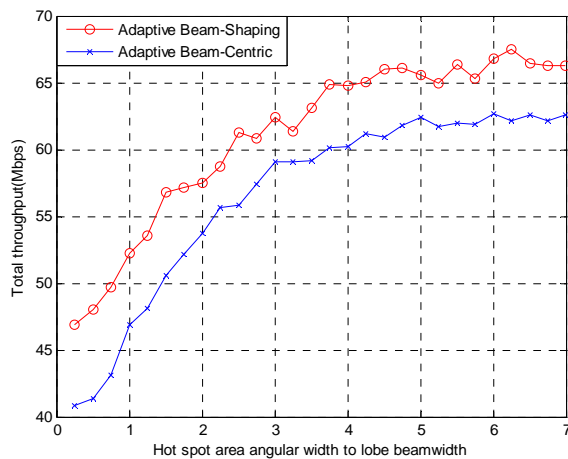


Fig. 9. Total throughput - Adaptive beam-centric AC strategy versus ABS strategy - 1 hotspot in the central cell.

VI. CONCLUSIONS

The performance of an adaptive beam-shaping strategy has been evaluated for WCDMA multicellular networks employing AAs at the central BS and up to the first tier of cells. Beamforming is performed by giving priority to the high data rate MSs, while at the same time fewer directional beams are formed overall in order to provide coverage to all other potential MSs.

Extensive MC simulations were performed in a network topology with up to four tiers of cells around the central cell. Due to the increased complexity of the simulations, as apart from the high number of effective sectors in the network up to 90% loading was considered in cells, simulations were performed in parallel with the use of a grid-enabled WCDMA system level simulator. Simulation scenarios included multirate services and various non-uniform traffic configurations which represent realistic traffic scenarios. Moreover, a hybrid statistical – deterministic propagation model was employed, in order to provide more accurate power estimations.

As shown in the results, the ABS strategy can achieve up to 75/120/165% throughput per beam gain for 1/2/3 hotspots per cell, respectively, in the first tier of cells by forming appropriate radiation patterns according to traffic demands. This gain is maximized for small hotspot area angular width and increased number of hotspots per cell, as in these cases there is increased spatial isolation among the MSs. Moreover, the gain can be up to 35% for uniform traffic distribution, while it is practically independent of the channel conditions.

The ABS strategy, apart from increased throughput per beam relatively to a fixed grid of beams sectorization strategy, also provides reduction in the interbeam handovers due to the decreased number of beams, which in turn results in reduced signaling requirements and easier network planning.

Ongoing research includes the extension of ray-tracing propagation modeling to all cells of the network, in the context of the grid-enabled simulator, as well as the development of a combined system-link level simulator for performance analysis and evaluation of advanced beamforming techniques in multicellular MIMO-WCDMA networks.

ACKNOWLEDGMENTS

The work presented in this paper has been funded by the project PENED 2003(03ED/226). The project is co-financed 75% of public expenditure through the EC - European Social Fund, 25% of public expenditure through the Ministry of Development-General Secretariat of Research and Technology and through the private sector, under measure 8.3 of operational program "COMPETITIVENESS" in the 3rd Community Support Program. The authors would like to thank Theodoros Athanaileas for the development of the grid-enabled WCDMA simulator. Finally, G. Athanasiadou wishes to thank Cambridge Broadband Ltd., Cambridge, UK, for the provision of the geographical databases.

REFERENCES

- [1] H. Holma and A. Toskala, Eds., *WCDMA for UMTS. Radio Access for Third Generation Mobile Communications*, 3rd ed, Wiley, 2004.
- [2] A. Czylik and A. Dekorsy, "System-level performance of antenna arrays in CDMA-based cellular mobile radio systems", *EURASIP Journal on Applied Signal Processing*, vol. 1, pp. 1308-1320, January 2004.
- [3] K. I. Pedersen and P. E. Mogensen, "Directional power based admission control for WCDMA systems using beamforming antenna array systems", *IEEE Trans. Veh. Technol.*, vol. 51, pp. 1294–1303, Nov. 2002.
- [4] M. Pausini et al., "Intelligent algorithms for user allocation and partial-adaptive beamforming in WCDMA uplink", in *proc. of ICC*, vol. 5, pp. 3341-3345, May 2003.
- [5] F. Adelantado J. P. Romero and O. Sallent, "Nonuniform traffic distribution model in reverse link of multirate/multiservice WCDMA-based systems", *IEEE Trans. Veh. Technol.*, vol. 56, pp. 2902–2914, September 2007.

- [6] T. V. Nguyen, P. Dassanayake, and M. Faulkner, "Use of adaptive sectorisation for capacity enhancement in CDMA cellular systems with non-uniform traffic," *Wireless Personal Communications Magazine*, vol. 28, pp. 107-120, January 2004.
- [7] J. Zhang, et al., "An efficient algorithm for adaptive cell sectoring in CDMA systems", in *proc. of ICC*, vol. 2, pp. 1238-1242, May 2003.
- [8] P. Gkonis, G. Tsoulos and D. I. Kaklamani, "An adaptive admission control strategy for WCDMA multicellular networks with non-uniform traffic", in *proc. of the 66th VTC*, vol. 1, pp. 989-993, October 2007, Baltimore, USA.
- [9] T. Athanaileas, P. Gkonis, G. Athanasiadou, G. Tsoulos and D. Kaklamani, "Implementation and evaluation of a web-based grid-enabled environment for WCDMA multibeam system simulations", *IEEE Antennas and Propagation Magazine*, vol. 50, pp. 195-204, June 2008.
- [10] 3GPP TR 25.996 v6.1.0, "Spatial Channel model for Multiple Input Multiple Output (MIMO) simulations", September 2003.
- [11] A. Goldsmith, *Wireless Communications*, Cambridge University Press, 2005.
- [12] G. E. Athanasiadou, "Incorporating the Fresnel zone theory in ray tracing propagation modelling of fixed wireless access channels", in *proc. of PIMRC*, vol. 1, pp. 1-5, September 2007, Athens, Greece.
- [13] K. Sipila, Z. Honkasalo, J. L. Steffens and A. Wacker, "Estimation of capacity and required transmission power of WCDMA downlink based on a downlink pole equation", in *proc. of the 51th VTC*, vol. 2, pp. 1002 – 1005, May 2000, Tokyo, Japan.
- [14] L.C. Godara, "Application of antenna arrays to mobile communications, Part II: Beam-forming and direction-of-arrival considerations," in *proc. of IEEE*, vol. 85, no. 8, pp. 1195-1245, August 1997.
- [15] K. I. Pedersen, P. E. Mogensen, and B. Fleury, "Spatial channel characteristics in outdoor environments and their impact on BS antenna system performance", in *proc. of the 48th VTC*, vol. 2, pp. 719-723, May 1998, Ottawa, Canada.
- [16] C. Chevallier, C. Brunner, A. Garavaglia, K. Murray and K. Baker, Eds., *WCDMA Deployment Handbook, Planning and Optimization Aspects*, Wiley Eds, 2006.

Panagiotis K. Gkonis was born in Athens, Greece in August 30, 1981. He received his Dipl.-Ing degree from the Electrical and Computer Engineering School of National Technical University of Athens (NTUA), Greece, in 2005. He is currently a candidate Ph.D. student in the School of Electrical and Computer Engineering of NTUA. His primary research interests include physical layer simulation techniques of cellular networks with adaptive antennas and MIMO systems.

George V. Tsoulos graduated from the National Technical University of Athens (NTUA), Athens, Greece, in 1992, and received his PhD degree from the University of Bristol, Bristol, UK, in 1997. From 1994 until 1999, he was a Research Associate/Fellow at the Centre for Communications Research of the University of Bristol. He then joined the Wireless Technology Practice of the PA Consulting Group, in Cambridge, UK. Between 2003 and 2004, he was with the Institute of Communication and Computer Systems, Athens, Greece, and he then joined the University of Peloponnese, Department of Telecommunications Science & Technology, Wireless & Mobile Communications Lab, where he is currently an Assistant Professor. His research interests include advanced wireless communications, smart antennas, and MIMO systems.

Georgia E. Athanasiadou graduated from the National Technical University of Athens (NTUA), Athens, Greece, in 1992, and received her PhD degree from the University of Bristol, UK in 1998. She was a Research Assistant and then a Research Fellow at the University of Bristol (1993-1999), and an Industrial Research Fellow at the University of Cambridge (2001- 2002). She has also worked as Senior Research Engineer at Adaptive Broadband Ltd., Cambridge, UK (1999-2001). Since 2002, she has been an Assistant Professor at the University of Peloponnese. Her research interests include radiowave propagation modeling and network planning.

Dimitra I. Kaklamani was born in Athens, Greece, in 1965. She received the PhD degree from the National Technical University of Athens (NTUA) in Electrical and Computer Engineering (ECE) in 1992. In April 1995, April 2000, and October 2004, she was elected Lecturer, Assistant Professor, and Associate Professor, respectively, in the School of ECE, NTUA. She has more than 200 publications in the fields of software development for information transmission systems modeling, microwave networks, and mobile and satellite communications. She has coordinated the NTUA activities in the framework of several EU and national projects in the same areas. She is an Editor of one international book by Springer-Verlag (2000) on applied CEM. Prof. Kaklamani is a reviewer for several IEEE journals.